BIOLOGICAL SCIENCES: Neuroscience

PPARγ-coactivator-1α gene transfer reduces neuronal loss and amyloid-β generation by reducing BACE1 in an Alzheimer's disease model

Short title: PGC-1α gene therapy for Alzheimer's disease

Loukia Katsouri[*], Yau M Lim[*], Katrin Blondrath[*], Ioanna Eleftheriadou[†], Laura Lombardero-Iturrizaga[*], Amy M Birch[*], Nazanin Mirzaei[*], Elaine E Irvine[‡], Nicholas D Mazarakis[†§] and Magdalena Sastre*[§]

[*]Centre for Neuroinflammation and Neurodegeneration, Division of Brain Sciences, Imperial College London, London W12 0NN, UK.

†Gene therapy, Division of Brain Sciences, Imperial College London, London W12 0NN, UK.

‡Institute for Clinical Sciences, MRC CSC, London W12 0NN, UK.

§To whom correspondence should be addressed: m.sastre@imperial.ac.uk; n.mazarakis@imperial.ac.uk; phone: +44-2075946673; Fax: +44-2075946548; Division of Brain Sciences, Hammersmith Hospital, Du Cane Road, London W12 0NN, UK

Abstract

Current therapies for Alzheimer's disease (AD) are symptomatic and do not target the underlying Aβ pathology and other important hallmarks including neuronal loss. PPARγ-coactivator-1α (PGC-1α) is a transcriptional regulator of metabolic genes, oxidative phosphorylation and mitochondrial biogenesis. We previously reported that PGC-1α also regulates the transcription of BACE1, the main enzyme involved in amyloid-β (Aβ) generation and its expression is decreased in Alzheimer's disease (AD) patients. We aimed to explore the potential therapeutic effect of PGC-1α by generating a lentiviral vector to express human PGC-1α and target it by stereotaxic delivery to hippocampus and cortex of APP23 transgenic mice at the preclinical stage of the disease. Four months post injection, APP23 mice treated with hPGC-1α showed improved spatial and recognition memory concomitant with a significant reduction in Aβ deposition, associated with a decrease in BACE1 expression. hPGC-1α overexpression attenuated the levels of pro-inflammatory cytokines and microglial activation. This effect was accompanied by a marked preservation of pyramidal neurons in the CA3 area and increased expression of neurotrophic factors. The neuroprotective effects were secondary to a reduction in Aβ pathology and neuroinflammation, because wild-type mice receiving the same treatment were unaffected. These results suggest that the selective induction of PGC-1α gene in specific areas of the brain is effective in targeting AD-related neurodegeneration and holds potential as therapeutic intervention for this disease.

Key words: Aβ/ BACE1/ growth factor/ inflammation/ neurodegeneration.

Significance statement

The PPARγ coactivator-1α (PGC-1α) is a transcriptional regulator of genes involved in energy metabolism. We observed previously that PGC-1α decreases the generation of Aβ in cell culture and its levels are reduced in Alzheimer's disease (AD) brains. To determine its potential therapeutic role *in vivo*, we delivered PGC-1α in specific brain areas of an AD model using viral vectors. We found that PGC-1α injected mice showed decreased Aβ plaques by reduced expression of the main enzyme involved in Aβ production, preserving most neurons in the brain and performing as well as wild-type mice in cognitive tests. Therefore, PGC1α selective delivery shows promising therapeutic value in AD.

/body

Introduction

Alzheimer's disease is the most prevalent form of dementia in the elderly and affects more than 40 million people worldwide (Alzheimer's net). The global cost of dementia is estimated at over 800 billion USD, without effective treatment that can at least halt, cure and prevent the disease (World Alzheimer's report 2015). Current drug therapies for Alzheimer's disease are merely symptomatic and do not target the underlying cause of the disease. New strategies include disease-modifying treatments, which aim to reduce the production of amyloid-β (Aβ) peptides and plaques or the modified protein tau and tangles. These are expected to block the progression of the disease and prevent neuronal loss, but are likely also to have serious side effects (1, 2).

We have recently explored the potential neuroprotective effects of the PPARγ-coactivator 1α (PGC-1α), a transcriptional co-activator for this nuclear receptor and for other transcription factors (3). PGC-1α is abundantly expressed in high-energy demanding tissues such as adipose tissue, liver, skeletal muscle, heart, kidney, and brain (4) where it is involved in the regulation of glucose and lipid metabolism, oxidative phosphorylation, and mitochondrial biogenesis (3, 5).

PGC-1α has been implicated in various neurodegenerative diseases (6) and its expression is reduced in the brain of Alzheimer's disease patients (7, 8). Interestingly, exogenous human PGC-1α expression in neuroblastoma cells and in primary neurons from the Tg2576 mouse model of Alzheimer's disease decreased Aβ generation and increased non-amyloidogenic sAPPα levels (7, 8). Additionally, we showed that PGC-1α mediates this effect by reducing BACE1 gene transcription via a PPARγ-dependent mechanism (7). Conversely, crossing Tg2576 with mice deficient in PGC-1α or silencing PGC-1α using siRNA transfection in neuronal cells, led to increased Aβ levels (7–9). Pharmacological stimulation of PGC-1α synthesis with nicotinamide riboside, the precursor of NAD^+, resulted in reduced Aβ levels and attenuated cognitive deterioration in Tg2576 mice (9). Furthermore, treatment with resveratrol, another PGC-1α activator, increased the activity of the Aβ degrading enzyme neprilysin and reduced amyloid plaques (10). Nevertheless, these drugs may promote these beneficial effects by acting on molecules other than PGC-1α, and an additional independent approach to investigate these specific functions of PGC-1α in Alzheimer's disease was therefore considered relevant. We hypothesized that gene therapy with PGC-1α delivered in brain could be neuroprotective because of its

effect on the transcription of genes involved in Aβ generation, energy and glucose metabolism and oxidative stress.

The aim of this study was to generate a lentiviral vector expressing human PGC-1α and target it in defined brain regions of APP23 transgenic mice by stereotaxic delivery, allowing us to evaluate the secific effects of this transcriptional regulator and define its potential for gene therapy for Alzheimer's disease. Our results show that PGC-1α prevents neuronal loss by increasing the transcription of growth factors and by decreasing Aβ-mediated neuroinflammation in those animals, consolidating the potential of PGC-1α gene delivery as treatment for Alzheimer's disease.

Manuscript text

Results

Effective transduction of PGC1α using RVG-B2c lentiviral vectors confers neurotropism and high expression in brain

Lentiviral vectors (LV) that efficiently transduce neurons were generated, compared by various combinations of gene promoters and viral envelope glycoproteins. We first tested vesicular stomatitis viral glycoprotein (VSVG) and rabies virus glycoprotein B2c (RVG). Pseudotyping lentiviral vectors with the RVG envelope glycoprotein confers both neurotropism and, more importantly, the ability of retrograde transport along neuronal axons (11). Additionally, we compared lentiviral vectors carrying the ubiquitous human CMV major immediate-early enhancer/promoter or the neuronal-specific human synapsin I (SYN) gene promoter. We generated combinations of VSVG-CMV, VSVG-SYN, RVG-CMV, and RVG-SYN vectors that carried the enhanced GFP (eGFP) gene and injected them unilaterally in the brain of wild-type mice. RVG-CMV resulted in higher expression, transduced cells both proximal and distal to the site of injection and preferentially transduced pyramidal neurons in the cortex and the CA1 area of the hippocampus (Fig S1G-L). CMV promoter was selected since it resulted in higher expression compared with the SYN promoter (Fig S1E-L, M). The neurotropism of the vector was confirmed by co-staining for eGFP and NeuN (Fig 1A-D) showing little or no localization of the transgene with astrocytes or microglia by co-staining of eGFP with Iba1 and GFAP (Fig 1E-H).

Therefore, the RVG-CMV-eGFP LV and RVG-CMV- hPGC-1α LV (further referred as LV-eGFP and LV-hPGC-1α) were generated as the vectors of choice (Fig 1I).

The efficiency of the lentiviral vectors LV-eGFP and LV-hPGC-1α injected in cortex and hippocampus (HIP) of wild-type and APP23 mice was measured four months post injection (p.i.). The expression of hPGC-1α protein in the brain of injected mice was evaluated by IHC using an antibody against the V5 tag, at the N-terminus of the hPGC-1α construct (Fig 1J). Moreover, *hPGC-1α* mRNA expression was confirmed by qRT-PCR analysis in the HIP, parietal cortex (Pt Ctx), and frontal cortex (Ft Ctx) of the injected APP23 mice (Fig 1K).

hPGC-1α gene delivery improves spatial and recognition memory in APP23 mice

We next determined the therapeutic effects of long-term overexpression of hPGC-1α in the cortex and hippocampus of wild-type and APP23 mice, delivering it at the age of eight months and lasting for four and a half months (Fig 2A). At eight months, female APP23 mice show first rare amyloid deposits, representing the pre-clinical stage of the disease (12–14). To assess any adverse effects, we monitored several parameters after surgery, including body weight, motility and anxiety (supplementary information).

To define whether chronic expression of LV-hPGC-1α in cortex and hippocampus of APP23 and wild-type mice affected their memory, behavioural tests were carried out four months p.i.. Spatial memory was evaluated by object location task (OLT), based on the spontaneous tendency of rodents to recognize an object that has been relocated and spend more time exploring it. The APP23 mice (at 12 months of age) that received the control vector displayed spatial memory deficits and were not able to discriminate between the displaced and the non-displaced object (Fig 2B). This was as expected because at this age APP23 mice exhibit memory decline, concomitantly with amyloid plaques (12, 15). Conversely, APP23 animals injected with LV-hPGC-1α showed no deficits in spatial memory and performed as well as the two groups of wild-type mice, all preferring the displaced object (Fig 2B). Following OLT, the mice were subjected to the novel object recognition test (NOR), which takes advantage of their exploratory behaviour and tendency to spend more time with a novel object over a familiar one. The results of the

NOR revealed that the APP23/LV-hPGC-1α mice were able to discriminate and explored for a longer time the novel object, while the APP23/LV-eGFP mice showed profound deficits (Fig 2B-C). It is worth noting that the expression of hPGC-1α in brain did not improve the performance of wild-type mice (Fig 2C). These combined results demonstrate that lentiviral mediated hPGC-1α expression prevented memory deficits in APP23 mice.

hPGC-1α chronic overexpression reduces BACE1, Aβ levels, and plaque load in APP23 mice

To quantify Aβ load by IHC we used a monoclonal Aβ-specific antibody that does not cross-react with full-length APP or CTFs (16). Histopathological examination revealed significantly lower Aβ burden in cortex (19.1% reduction) and hippocampus (30% reduction) in APP23/LV-hPGC-1α mice compared with animals injected with the control vector (Fig 3A-C). Plaque burden was quantified after brain sections were stained with AmyloGlo, instead of the standard Thioflavin-S dye, because this interfered with eGFP detection (17). We observed that the area covered by amyloid plaques was decreased in the APP23/LV-hPGC-1α mice, both in cortex and hippocampus compared to the APP23/LV-eGFP mice (43% and 51% decrease respectively) (Fig 3D-F). Western blot analysis of brain homogenates confirmed the immunohistological results, showing reduced Aβ levels in the APP23/LV-hPGC-1α mice compared with APP23 mice treated with control vector (Fig 3G-I). In addition, ELISA for $A\beta_{40}$ and $A\beta_{42}$ subtypes in the same samples corroborated these results (Fig 3J). No alterations were found in the expression of the precursor protein APP by PGC-1α gene delivery (Fig 3K). Our previous *in vitro* studies demonstrated that increased PGC-1α expression reduces *Bace1* transcription (7). In line with those *in vitro* results, the brain levels of β-CTF and sAPPβ, the main products of BACE1, were remarkably reduced in APP23 mice that received LV-hPGC-1α compared to APP23 injected with LV-eGFP (Fig 3L). . In complete agreement, the chronic expression of hPGC-1α in the brain of APP23 mice lowered BACE1 protein levels compared with control mice (Fig 3M-N). Interestingly, an inverse correlation between hPGC-1α and *Bace1* mRNA levels indicated lower *Bace1* mRNA expression to be associated with higher PGC-1α levels (Fig 3O), Pearson's $r=-0.7255$, $P<0.05$). Furthermore, overexpression of hPGC-1α affected the expression of other secretases, e.g. higher *Adam17* mRNA levels (Fig 3P). Although no major changes were detected in sAPPα and αCTFs, the products of α-

secretase, the ratio sAPPα/sAPPβ was found strongly increased, indicating a shifting in the balance towards α-secretase No significant alterations were observed in the Aβ clearance or degradation mechanisms (Fig S3). Together, our combined data demonstrate that LV-hPGC-1α CNS transduction resulted in higher levels of human PGC-1α triggering a robust reduction of Aβ production and plaque formation, however not by affecting Aβ clearance or degradation.

hPGC-1α attenuates neuroinflammation in APP23 mice

The APP23 mouse model of brain amyloidopathy exhibits a strong neuroinflammatory component (12–15). We quantified the density of microglia and astrocytes in areas surrounding amyloid plaques of similar size. Microglial activation was detected by IHC for Iba-1 and found attenuated in APP23 injected with LV-hPGC-1α compared with animals injected with control vector both in cortex and hippocampus (Fig 4, A, B, D-F, H-J). We did not observe major changes in astrocytosis surrounding the plaques, detected by GFAP staining (Fig 4, A, C-E, G-H, K-L), although total GFAP expression was reduced in hippocampal homogenates of APP23/LV-hPGC-1α mice (Fig 4M). Importantly, the expression of the main pro-inflammatory cytokines TNF-α and IL-1β were significantly reduced in the APP23/LV-hPGC-1α mice compared to the APP23/LV-eGFP mice (Fig 4N-O), whereas no significant changes were observed for IL-6, IL-10 and MCP-1 (Fig 4P-R). In summary, hPGC-1α affects the activation of microglia, reducing their pro-inflammatory profile.

hPGC-1α prevents neuronal loss in the hippocampus of APP23 mice

APP23 mice suffer neuronal loss in specified hippocampal areas at age 12 months (18) and was confirmed by immunohistochemical analysis with NeuN in brains of APP23/LV-eGFP mice, showing a 30% reduction in neuronal number in the CA3, compared to wild-type/LV-eGFP mice (Fig 5A-J). Remarkably, in APP23 mice treated with LV-hPGC-1α we observed a marked preservation of pyramidal neurons in the CA3 (Fig 5, C, F, and I), consistent with the absence of memory impairment described above. We found no significant changes in neuronal density in the dentate gyrus and subiculum in LV-hPGC-1α injected mice (Fig 5J and Fig. S4), suggesting that the neuroprotective effect was not linked to increased neurogenesis. In addition, PGC-1α gene delivery did not alter

neuronal count in the brains of wild-type mice, indicating that the positive effect on neurons was associated with reduced amyloid load and pathology (Fig 5, I-J).

This conclusion was further supported by data showing increased mRNA expression of the neuroprotective factor *Bdnf* (Fig 5K) and the levels of the post-synaptic protein PSD-95 only in APP23/LV-hPGC-1α and not in wild-type mice (Fig 5M). Interestingly, the expression of *Ngf* was found increased in both wild-type and APP23 mice overexpressing hPGC-1α.

Discussion

The present study shows that gene delivery of hPGC-1α in the brain of transgenic APP mice reduced amyloid deposition, improved memory and prevented neuronal loss. Importantly, we describe a potential treatment that can preserve neuronal viability and improve memory in AD corroborating other neuroprotective approaches, such as gene therapy with growth factors. This was recently highlighted in Alzheimer's disease patients treated with NGF gene delivery, which revealed increased axonal sprouting, cell hypertrophy, and activation of functional markers (19).

The observed PGC-1α-mediated positive effects, however, do not seem to involve alterations in neuronal proliferation, as the preservation of dentate gyrus integrity, an area directly involved in neurogenesis, remained unchanged by LV-hPGC-1α. Most interestingly, increased expression of neurotrophic factors NGF and BDNF was evident following LV-hPGC-1α gene therapy and both exert neuroprotective properties in Alzheimer's disease (20, 21). In line with our findings was the recent report showing that exercise-induced BDNF expression was mediated by PGC-1α regulation of Fndc5 gene expression (22). Moreover, PPARγ and PPARα, the main transcription factors regulated by PGC-1α, induced the transcription of BDNF in cultured neurons and glial cells (23) Roy et al., 2015, Cell Metabolism 22, 1–13. Combined, these data are fully consistent with a mechanism for the neuroprotective effects of hPGC-1α in APP23 mice mediated, at least partially, by increased transcription of specific growth factors (Fig S5K). Consistent with our results, previous work demonstrated that PGC-1α knockout mice develop neurological abnormalities and show prominent neurodegeneration (24, 25).

In addition, our data indicate that the beneficial effects on memory and neurodegeneration are a consequence of the reduction in Aβ generation and the associated inflammatory response, because memory and neuronal numbers were not affected in wild-type mice that received the same LV-hPGC-1α treatment. Therefore, the therapeutic effect of PGC-1α required a pro-inflammatory state in order to be effective, in this case evidently caused by hAPP overexpression and Aβ production in the APP23 mice (Fig. S5K). Furthermore, because we found that hPGC-1α was mostly expressed in neurons, we presume that the anti-inflammatory reaction observed by hPGC-1α delivery in the brain is secondary to the decrease on Aβ levels produced by neurons, since Aβ is able to induce a pro-inflammatory reaction in the brain (Sastre et al., 2006). Our results do not support a noticeable involvement of enhanced mitochondrial function (see supplementary information and Fig. S5) or the autophagy/lysosomal pathway in the neuroprotective effects of PGC-1α in APP23, as previously suggested in other neurological disease models, such as Huntington's disease (26).

A recent study of a bigenic model obtained crossing the Tg19959 with PGC-1α transgenic mice reported reductions in the levels of Aβ40 by ELISA, while increased Congo red staining for aggregated Aβ. The results of this publication were obtained from a transgenic mouse overexpressing elevated levels of PGC-1α under a promoter not specific for a particular cell type, and consequently the results do not necessarily have to coincide with our model, in which the gene is expressed for only 4 months in certain brain areas (27). Indeed, sustained high overexpression of PGC-1α produced toxic effects in muscles and heart, caused or accompanied by extensive mitochondrial proliferation and by myopathy (28, 29). Extremely high levels of PGC-1α achieved with adenoviral vectors also resulted in deleterious effects in dopaminergic neurons, in susbtantia nigra (30, 31) as opposed to the striatum, where 4-fold higher levels were not toxic, in mouse models of Hungtinton's and Parkinson's disease (32, 33). The different outcomes in different studies must relate to the fact that dopaminergic neurons are more susceptible to degeneration from oxidative damage than other neuronal subtypes and suggest that selective delivery in specific brain regions is necessary to achieve beneficial effects. The lentiviral vector for delivery of hPGC-1α in our study was well tolerated, did not trigger adverse effects and allowed sustained expression of the transgene for months. Successful proof-of-principle studies of gene therapy using

similarly pseudotyped lentiviral vectors have been demonstrated in animal models of ALS (34, 35), spinal muscular atrophy (36), and spinal nerve injury (37). In addition, we have developed and tested a similar vector for dopamine replacement therapy in late stage Parkinson's disease patients in a phase I/II clinical trial, showing long-term expression and improved motor behavior in treated patients (38). We believe, therefore, that future innovations in gene therapy provide hope and clinical potential also in Alzheimer's dementia. Although this method of delivery is at this time invasive and therefore has some translational limitations, our data provide a proof of concept for future drug discovery programs aimed to induce the PGC-1α gene to target neurodegeneration.

Materials and Methods

Animals

Eight months old female APP23 mice (Novartis) and wild-type littermates (C57Bl/6) were used. APP23 mice express the hAPP cDNA carrying the Swedish mutation under the control of the neuronal specific Thy1.2 promoter and are characterized by amyloid deposition, plaque formation, neuroinflammation, neuronal loss, and memory deficits (12, 13). All the animals were kept in individually ventilated cages in a 12/12h light/dark cycle with controlled temperature and humidity and food and water ad libitum. The experiments were designed in compliance with the UK Home Office and Imperial College London's ethical committees approved the present study.

Lentiviral vectors and injections

Recombinant non-replicative HIV-1-based lentiviral vectors (LV) were produced based on the standard four-plasmid transfection of HEK-293T cells as previously described (39) (see supplementary information).

Immunohistochemistry and immunofluorescence

All the antibodies were incubated overnight at 4^{o} C (anti-Aβ MOAB-2 1:1000, anti-V5 1:500, and anti-NeuN, 1:500) in 2 % FBS in TBS-Tx 0.02%. Subsequent developing steps were performed as described previously(15). For immunofluorescent stainings, sections were incubated with AmyloGlo (Biosensis, Australia) and primary antibodies against eGFP (Abcam), Iba1 (Wako), GFAP (Invitrogen) at a 1:500 dilution and NeuN (Millipore, dilution 1:400) overnight at 4^{o}C and detected with secondary fluorescent

antibodies at a 1:400 dilution (AlexaFluor dyes, Invitrogen). Images were captured using a Leica SP5 Confocal microscope.

Western blotting

Western blot analysis was carried out as described (15) using antibodies against Aβ (clone 6E10, Covance), BACE1 (Cell Signalling), PSD-95 and IDE (Abcam), COX-4 (kind gift from Dr. Kambiz Alavian), hPGC-1α (Santa Cruz) and LC3 (Abcam) used at a 1:1000 dilution, R1(57) (kind gift from Dr P. Mehta, New York) at a 1:2000 dilution and 140 (from Jochen Walter, Bonn) against CT-of APP; Neprilysin (Millipore),APOE and hPGC-1α (Santa Cruz) at a 1:500 dilution, V5 (Invitrogen) at a 1:5,000 and LRP-1 (kind gift from Professor Claus Pietrzik, University Mainz) and β-actin (Abcam) at a 1:10,000 dilution. The intensity of the bands was quantified by densitometry using Image J software and sample loading was normalized to β-actin.

ELISAs

The levels of human Aβ42 were determined using a High Sensitivity Human Amyloid β42 ELISA kit (Millipore). For the mouse cytokines we used kits from Preprotech.

RNA extraction and quantitative RT-PCR

Tissues were lysed and homogenized in TRIzol reagent (Ambion) and total RNA was isolated using the RNeasy mini kit (Qiagen). First-strand cDNA was generated using Taqman reverse transcription reagents (Applied Biosystems) for Taqman Probes or QuantiTect Reverse Transcription kit (Qiagen) for custom-made primers. qPCR was performed using Taqman universal PCR mastermix or Quantifast SYBR green in a 7900HT real-time PCR system (Applied Biosystems). mRNA quantities were normalized to Gapdh after determination by the comparative Ct method. All samples were run in duplicates.

Statistical analysis

All data were checked for normal distribution using the Kolmogorov-Smirnov normality test, the Levene median test to ensure that variances are equal, and the Mauchly test of sphericity before performing the appropriate statistical analysis. The data were analysed with GraphPad Prism v6 and SPSS v20 (IBM) using two-tailed Student's *t-test* or Mann-Whitney test, two-way ANOVA followed

by Bonferroni post hoc analysis and correlation analysis. Power analysis was performed using GPower 3.0. All data in bar charts show means ± SEM. Differences were considered significant for $P<0.5$.

Footnotes

*Centre for Neuroinflammation and Neurodegeneration, Division of Brain Sciences, Imperial College London, London W12 0NN, UK.

†Gene therapy, Division of Brain Sciences, Imperial College London, London W12 0NN, UK.

‡Institute for Clinical Sciences, MRC CSC, London W12 0NN, UK.

§To whom correspondence should be addressed: m.sastre@imperial.ac.uk; n.mazarakis@imperial.ac.uk; phone: +44-2075946673; Fax: +44-2075946548; Division of Brain Sciences, Hammersmith Hospital, Du Cane Road, London W12 0NN, UK

Acknowledgements

The authors thank Dr Matthias Staufenbiel and the Novartis Institutes for Biomedical Research Basel for providing the APP23 mouse line for this study. We would like to thank Antonio Trabalza for initial training in stereotaxic surgeries, James Hislop (University of Aberdeen) for advice in cloning, Prof. Claus Pietrzik (University of Mainz) for anti-LRP1 antibody, Prof. James Uney (University of Bristol) for the lentiviral vector constructs, Dr Aikaterini Kralli for the PGC-1α cDNA plasmid (The Scripps Institute) and Prof. Fred Van Leuven (University of Leuven) for critical reading of the manuscript. This research was funded by Alzheimer's research UK (ART-PG2009-5, and ARUK-ESG-2013-8) to MS and ERC Advanced Investigators Programme Grant 23314 to NDM.

References

1. Galimberti D, Scarpini E (2011) Alzheimer's disease: from pathogenesis to disease-modifying approaches. *CNS Neurol Disord Drug Targets* 10(2):163–74.
2. Vassar R (2014) BACE1 inhibitor drugs in clinical trials for Alzheimer's disease. *Alzheimers Res Ther* 6(9):89.
3. Puigserver P, Spiegelman BM (2003) Peroxisome proliferator-activated receptor-gamma coactivator 1 alpha (PGC-1 alpha): transcriptional coactivator and metabolic regulator. *Endocr Rev* 24(1):78–90.
4. Tritos NA, et al. (2003) Characterization of the peroxisome proliferator activated receptor coactivator 1 alpha (PGC 1α) expression in the murine brain. *Brain Res* 961(2):255–260.
5. Austin S, St-Pierre J (2012) PGC1α and mitochondrial metabolism--emerging concepts and relevance in ageing and neurodegenerative disorders. *J Cell Sci* 125(Pt 21):4963–71.

6. Katsouri L, Blondrath K, Sastre M (2012) Peroxisome proliferator-activated receptor-γ cofactors in neurodegeneration. *IUBMB Life* 64(12):958–964.

7. Katsouri L, Parr C, Bogdanovic N, Willem M, Sastre M (2011) PPARγ co-activator-1α (PGC-1α) reduces amyloid-β generation through a PPARγ-dependent mechanism. *J Alzheimers Dis* 25(1):151–162.

8. Qin W, et al. (2009) PGC-1alpha expression decreases in the Alzheimer disease brain as a function of dementia. *Arch Neurol* 66(3):352–61.

9. Gong B, et al. (2013) Nicotinamide riboside restores cognition through an upregulation of proliferator-activated receptor-γ coactivator 1α regulated β-secretase 1 degradation and mitochondrial gene expression in Alzheimer's mouse models. *Neurobiol Aging* 34(6):1581–1588.

10. Karuppagounder SS, et al. (2009) Dietary supplementation with resveratrol reduces plaque pathology in a transgenic model of Alzheimer's disease. *Neurochem Int* 54(2):111–8.

11. Mazarakis ND, et al. (2001) Rabies virus glycoprotein pseudotyping of lentiviral vectors enables retrograde axonal transport and access to the nervous system after peripheral delivery. *Hum Mol Genet* 10(19):2109–2121.

12. Sturchler-Pierrat C, et al. (1997) Two amyloid precursor protein transgenic mouse models with Alzheimer disease-like pathology. *Proc Natl Acad Sci* 94(24):13287–13292.

13. Bondolfi L, et al. (2002) Amyloid-associated neuron loss and gliogenesis in the neocortex of amyloid precursor protein transgenic mice. *J Neurosci* 22(2):515–522.

14. Katsouri L, et al. (2013) Prazosin, an α(1)-adrenoceptor antagonist, prevents memory deterioration in the APP23 transgenic mouse model of Alzheimer's disease. *Neurobiol Aging* 34(4):1105–15.

15. Katsouri L, et al. (2015) Systemic administration of fibroblast growth factor-2 (FGF2) reduces BACE1 expression and amyloid pathology in APP23 mice. *Neurobiol Aging* 36(2):821–31.

16. Youmans KL, et al. (2012) Intraneuronal Aβ detection in 5xFAD mice by a new Aβ-specific antibody. *Mol Neurodegener* 7(1):8.

17. Schmued L, et al. (2012) Introducing Amylo-Glo, a novel fluorescent amyloid specific histochemical tracer especially suited for multiple labeling and large scale quantification studies. *J Neurosci Methods* 209(1):120–6.

18. Calhoun ME, et al. (1998) Neuron loss in APP transgenic mice. *Nature* 395(6704):755–756.

19. Tuszynski MH, et al. (2015) Nerve Growth Factor Gene Therapy: Activation of Neuronal Responses in Alzheimer Disease. *JAMA Neurol*. doi:10.1001/jamaneurol.2015.1807.

20. Aloe L, Rocco ML, Bianchi P, Manni L (2012) Nerve growth factor: from the early discoveries to the potential clinical use. *J Transl Med* 10(1):239.

21. Nagahara AH, et al. (2013) Early BDNF Treatment Ameliorates Cell Loss in the Entorhinal Cortex of APP Transgenic Mice. *J Neurosci* 33(39):15596–15602.

22. Wrann CD, et al. (2013) Exercise induces hippocampal BDNF through a PGC-1α/FNDC5 pathway. *Cell Metab* 18(5):649–659.

23. Kariharan T, et al. (2015) Central activation of PPAR-gamma ameliorates diabetes induced cognitive dysfunction and improves BDNF expression. *Neurobiol Aging* 36(3):1451–61.

24. Leone TC, et al. (2005) PGC-1alpha deficiency causes multi-system energy metabolic derangements: muscle dysfunction, abnormal weight control and hepatic steatosis. *PLoS Biol* 3(4):e101.

25. Lin J, et al. (2004) Defects in adaptive energy metabolism with CNS-linked hyperactivity in PGC-1alpha null mice. *Cell* 119(1):121–35.

26. Tsunemi T, et al. (2012) PGC-1α rescues Huntington's disease proteotoxicity by preventing oxidative stress and promoting TFEB function. *Sci Transl Med* 4(142):142ra97.

27. Dumont M, et al. (2014) PGC-1α overexpression exacerbates β-amyloid and tau deposition in a transgenic mouse model of Alzheimer's disease. *FASEB J* 28(4):1745–1755.

28. Miura S, et al. (2006) Overexpression of Peroxisome Proliferator-Activated Receptor γ Co-Activator-1α Leads to Muscle Atrophy with Depletion of ATP. *Am J Pathol* 169(4):1129–1139.

29. Russell LK (2004) Cardiac-Specific Induction of the Transcriptional Coactivator Peroxisome Proliferator-Activated Receptor Coactivator-1 Promotes Mitochondrial Biogenesis and Reversible Cardiomyopathy in a Developmental Stage-Dependent Manner. *Circ Res* 94(4):525–533.

30. Ciron C, Lengacher S, Dusonchet J, Aebischer P, Schneider BL (2012) Sustained expression of PGC-1α in the rat nigrostriatal system selectively impairs dopaminergic function. *Hum Mol Genet* 21(8):1861–1876.

31. Clark J, et al. (2012) Pgc-1α overexpression downregulates Pitx3 and increases susceptibility to MPTP toxicity associated with decreased Bdnf. *PLoS One* 7(11):e48925.

32. Cui L, et al. (2006) Transcriptional Repression of PGC-1α by Mutant Huntingtin Leads to Mitochondrial Dysfunction and Neurodegeneration. *Cell* 127(1):59–69.

33. St-Pierre J, et al. (2006) Suppression of Reactive Oxygen Species and Neurodegeneration by the PGC-1 Transcriptional Coactivators. *Cell* 127(2):397–408.

34. Ralph GS, et al. (2005) Silencing mutant SOD1 using RNAi protects against neurodegeneration and extends survival in an ALS model. *Nat Med* 11(4):429–33.

35. Azzouz M, et al. (2004) VEGF delivery with retrogradely transported lentivector prolongs survival in a mouse ALS model. *Nature* 429(6990):413–417.

36. Azzouz M, et al. (2004) Lentivector-mediated SMN replacement in a mouse model of spinal muscular atrophy. *J Clin Invest* 114(12):1726–1731.

37. Wong L-F, et al. (2006) Retinoic acid receptor beta2 promotes functional regeneration of sensory axons in the spinal cord. *Nat Neurosci* 9(2):243–50.

38. Palfi S, et al. (2014) Long-term safety and tolerability of ProSavin, a lentiviral vector-based gene therapy for Parkinson's disease: a dose escalation, open-label, phase 1/2 trial. *Lancet (London, England)* 383(9923):1138–46.

39. Eleftheriadou I, Trabalza A, Ellison S, Gharun K, Mazarakis N (2014) Specific retrograde transduction of spinal motor neurons using lentiviral vectors targeted to presynaptic NMJ receptors. *Mol Ther* 22(7):1285–98.

Figure legends

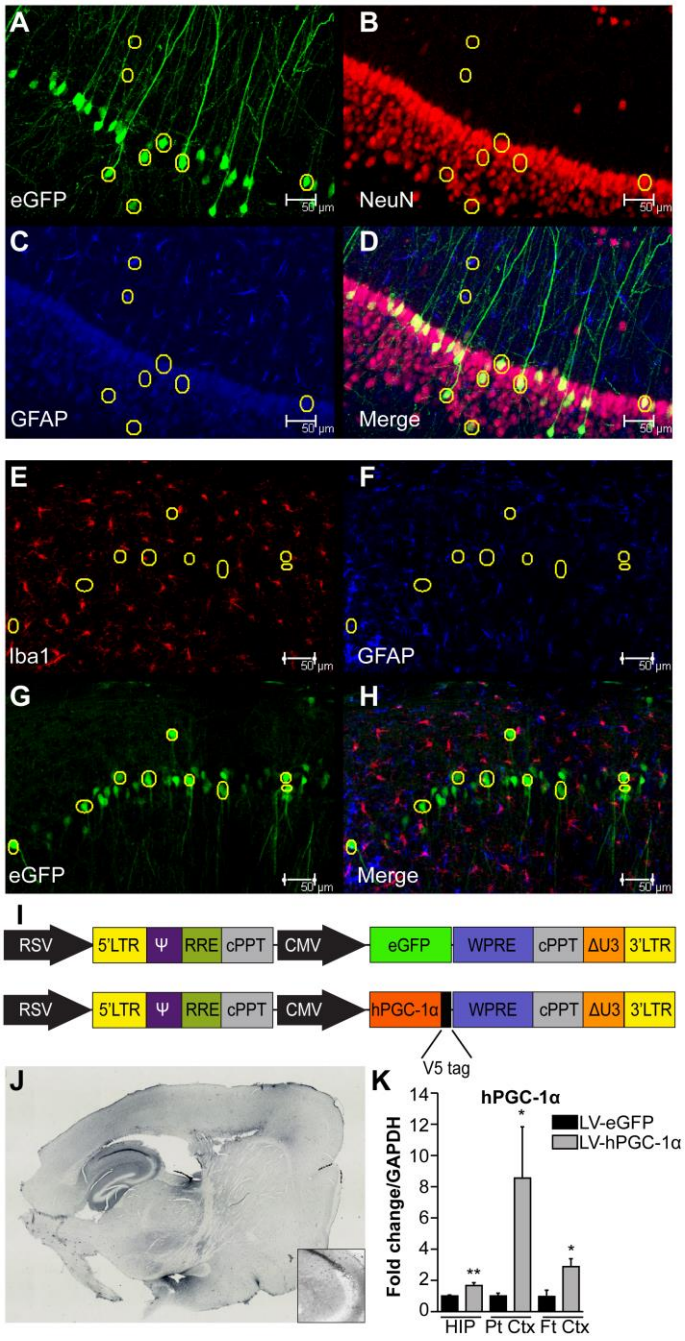

Figure 1

RVG-CMV lentiviral vector confers high transgene expression in neurons of hPGC-1α lentiviral-injected mice. (*A-D*) Representative images for eGFP (green), NeuN (red) and GFAP (blue) from RVG-CMV-eGFP injected wild-type mice showing clear co-localisation of NeuN and eGFP and very little or no co-localisation of eGFP with GFAP. Scalebar 50µm. (*E-H*) Representative images showing very low co-localisation with microglia (Iba1-red) or astrocytes (GFAP-blue) with the transgene (eGFP-green) in RVG-CMV-eGFP injected APP23 brains. Scalebar 50µm. (*I*) Schematic of the genome plasmids

used to generate the lentiviral (LV) vectors that were injected in the brains of wild-type and APP23 mice. The upper construct represents the pRRL-sincppt-CMV-eGFP-WPRE and the lower one the pRRL-sincppt-CMV-hPGC-1α-WPRE lentiviral genome plasmids. (*J*) Anti-V5 immunohistochemistry in a LV-hPGC-1α-injected mouse 4.5 months p.i. confirmed expression of the transgene in cortex and hippocampus. (*K*) Quantitative mRNA analysis by quantitative reverse transcriptase PCR analysis (qRT-PCR) for hPGC-1α showed increased expression in hippocampus (HIP; n=6), parietal cortex (Pt Ctx; n=7) and frontal cortex (Ft Ctx; n=5) of LV-hPGC-1α injected APP23 compared to the APP23/LV-eGFP mice 4 months p.i. *P<0.05, **P<0.01 two-tailed Student's t-test. Data are shown as mean±SEM.

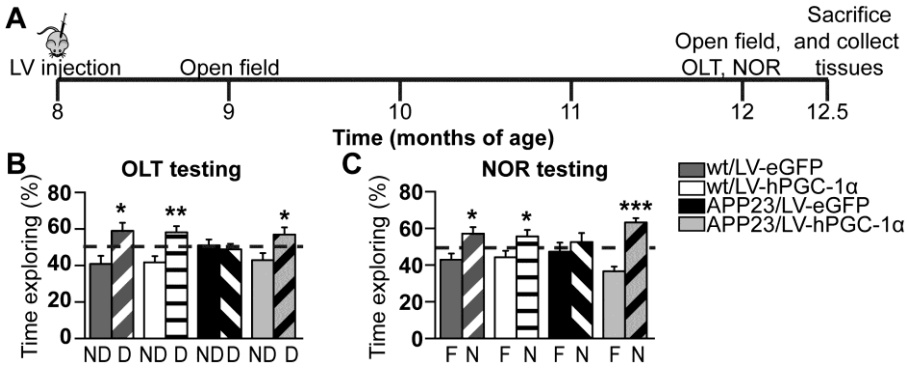

Figure 2

Cortical and hippocampal expression of hPGC-1α prevents memory decline in APP23 mice. (*A*) Schematic representation of the experimental procedure. Female mice were injected at eight months of age and behavioral tests were carried out 1 months and 4 months p.i. Tissues were harvested 4.5 months p.i. (*B*) APP23/LV-hPGC-1α mice at the age of 12 months (4 months post-surgery) had intact spatial memory assessed by Object location task (OLT) whereas the APP23/LV-eGFP injected mice showed memory deficits. The shaded columns show the displaced object (D) and the non-shaded the non-displaced object (ND) (*C*) NOR testing session showing that the APP23/LV-hPGC-1α mice had recognition memory values similar to the wild-type levels, while the APP23/LV-eGFP were unable to discriminate between the novel (labeled N, shaded columns) and the familiar object (labeled F) (n=8-10 per group) Two-tailed Student's t-test, *P<0.05, **P<0.01; *** P<0.001. Data are shown as mean±SEM.

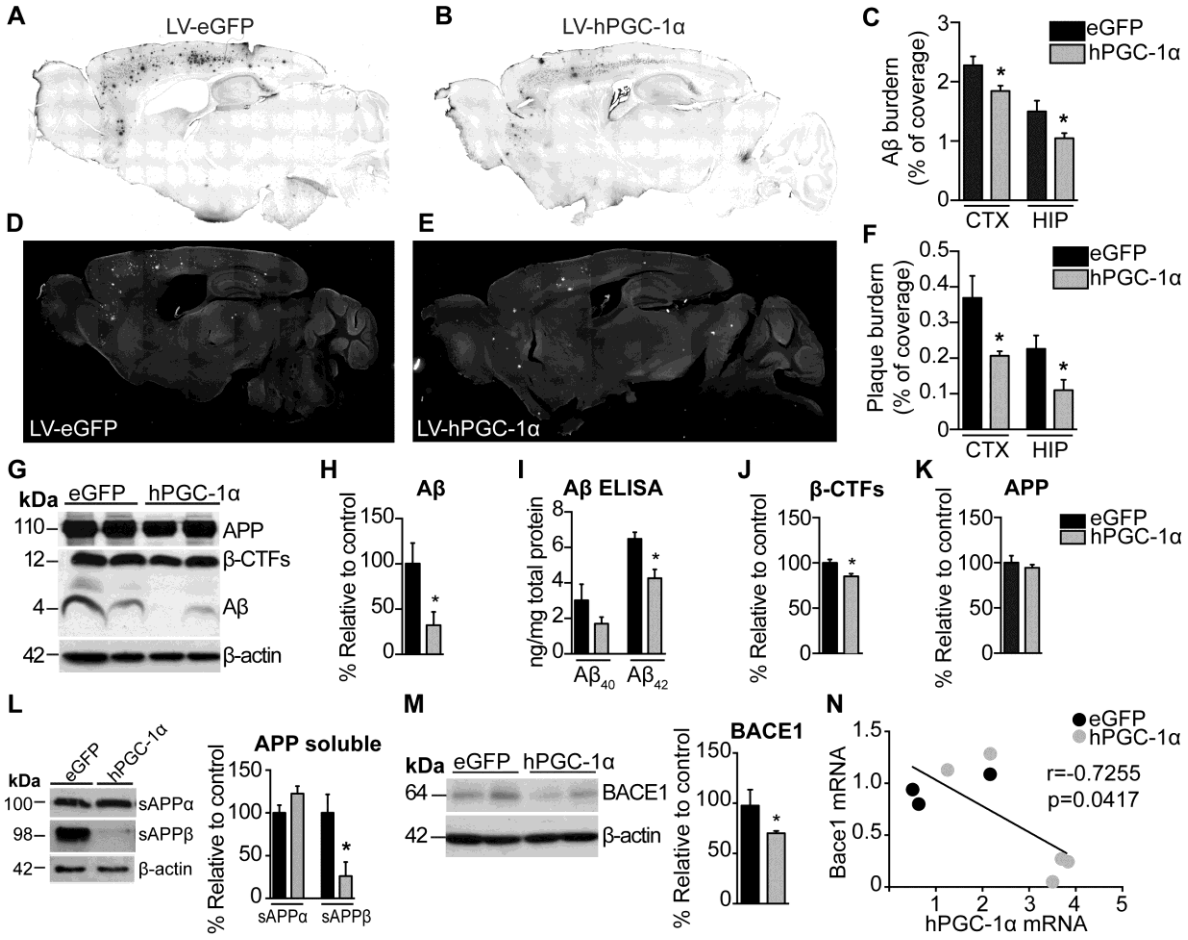

Figure 3

Cortical and hippocampal sustained expression of hPGC-1α decreases amyloid and plaque load in APP23 mice. (*A-B*) Representative images of anti-Aβ (MOAB-2) immunostained sections of APP23 injected with LV-eGFP and LV-hPGC-1α respectively. (*C*) Quantification of percentage of Aβ burden from MOAB-2 staining revealed a significant decrease in Aβ load in both the cortex and hippocampus of LV-hPGC-1α/APP23 mice compared to the LV-eGFP/APP23 (n= 9 per group). (*D-E*) Representative sections stained with AmyloGlo of APP23 injected with LV-eGFP and LV-hPGC-1α respectively and quantification of percentage of plaque burden (*F)* revealed a significant decrease in plaque load in LV-hPGC-1α/APP23 mice (n= 9, 7 sections per mouse). Representative western blots for Aβ from frontal cortices (*G*) and hippocampi (*H*) and their quantification (*I*) demonstrated that hPGC-1α overexpression decreased total Aβ (n= 5 per group). (*J*) ELISA for $A\beta_{42}$ in frontal cortex homogenates confirmed the reduction in Aβ in LV-hPGC-1α/APP23 mice (n= 4 to 5). (*K-L*) Quantification from G and H showed reductions in β-CTFs levels while full length APP expression was unchanged APP23/LV-PGC-1α (n=

5 for each group). (*M-N*) Representative western blot for BACE1 and quantification revealed a 25% reduction in BACE1 protein in the frontal cortex of LV-hPGC-1α/APP23 (n=5 for each group), (*O*) Correlation analysis of BACE1 mRNA and hPGC-1α mRNA showing a statistically significant inverse correlation between the two (Pearson's r=−0.7255, *P*=0.0417). (*P*) Adam17 mRNA levels were significantly increased in the cortex of LV/hPGC-1α APP23 mice compared to APP23/LV-eGFP. Hippocampus (HIP; n= 6), parietal cortex (Pt Ctx; n= 7) and frontal cortex (Ft Ctx; n= 5). **P*<0.05, ***P*<0.01 two-tailed Student's *t-test*. Data are shown as mean±SEM.

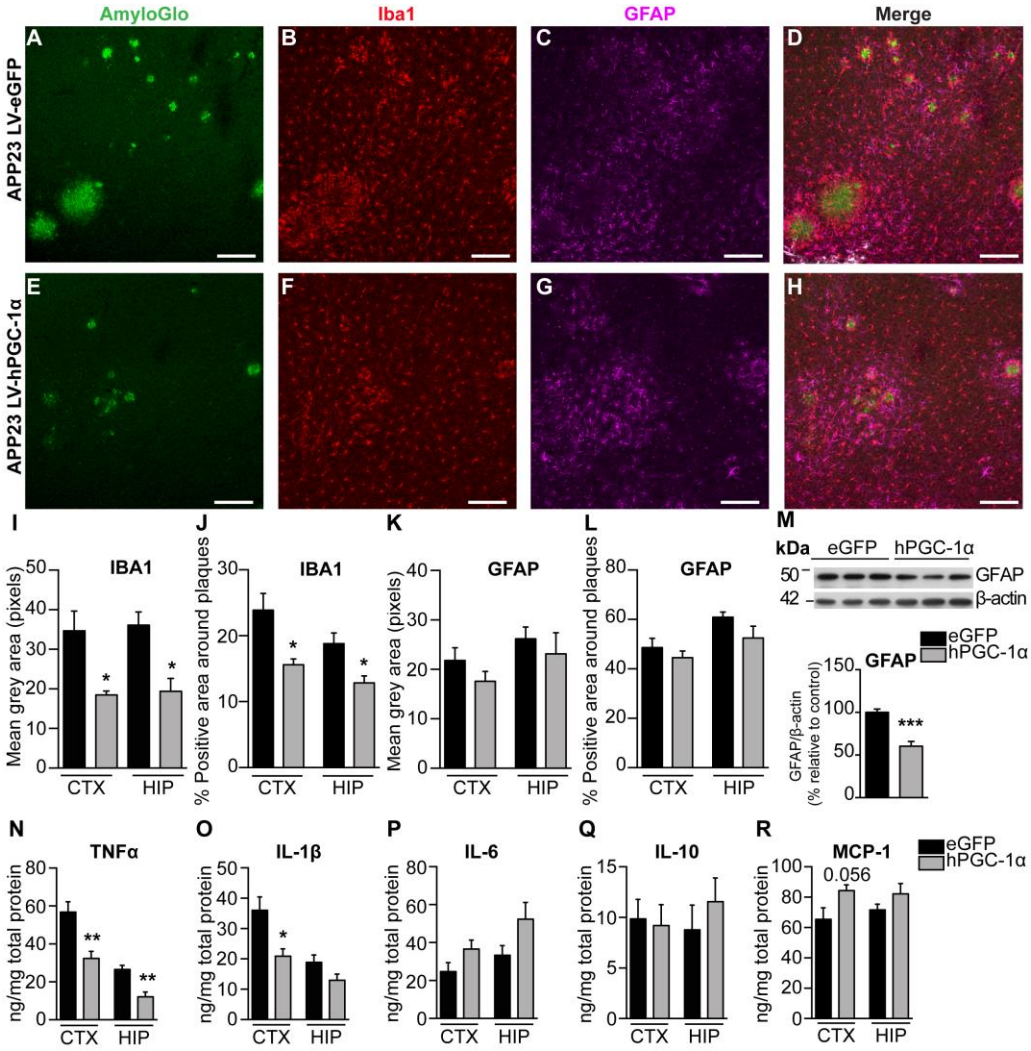

Figure 4.

LV-hPGC-1α gene delivery in cortex and hippocampus of APP23 mice reduces neuroinflammation. (*A-H*) Representative images of confocal imaging of triple staining for AmyloGlo (green), Iba1 (red) and GFAP (magenta) in LV-eGFP (*A-D*) and LV-hPGC-1α injected APP23 mice (*E-H*); n=5 per group, scalebars 250µm. Quantification of mean grey area (*I*) and % of coverage by microglial cells (*J*) in a

50μm^2 circular area surrounding the plaques showed a marked reduction of microglial activation in the APP23 mice LV-hPGC-1α (n= 5, 4 sections per mouse). GFAP-positive astrocytes surrounding the plaques quantified in 100μm^2 diameter circular areas quantified as mean grey area (*K*) or % of coverage (*L*) (n= 5, 4 sections per mouse). (*M*) Representative western blot in total hippocampal homogenates and quantification of GFAP (n= 5 for each group). (*N-R*) ELISAs for cytokines TNF-α (*N*), IL-1β (*O*) IL-6 (*P*), IL-10 (*Q*) and MCP-1 (*R*) in the frontal cortices and hippocampi (n= 5 for each group). *P<0.05, **P<0.01, ***P<0.001 two-tailed Student's t-test. Data are shown as mean±SEM.

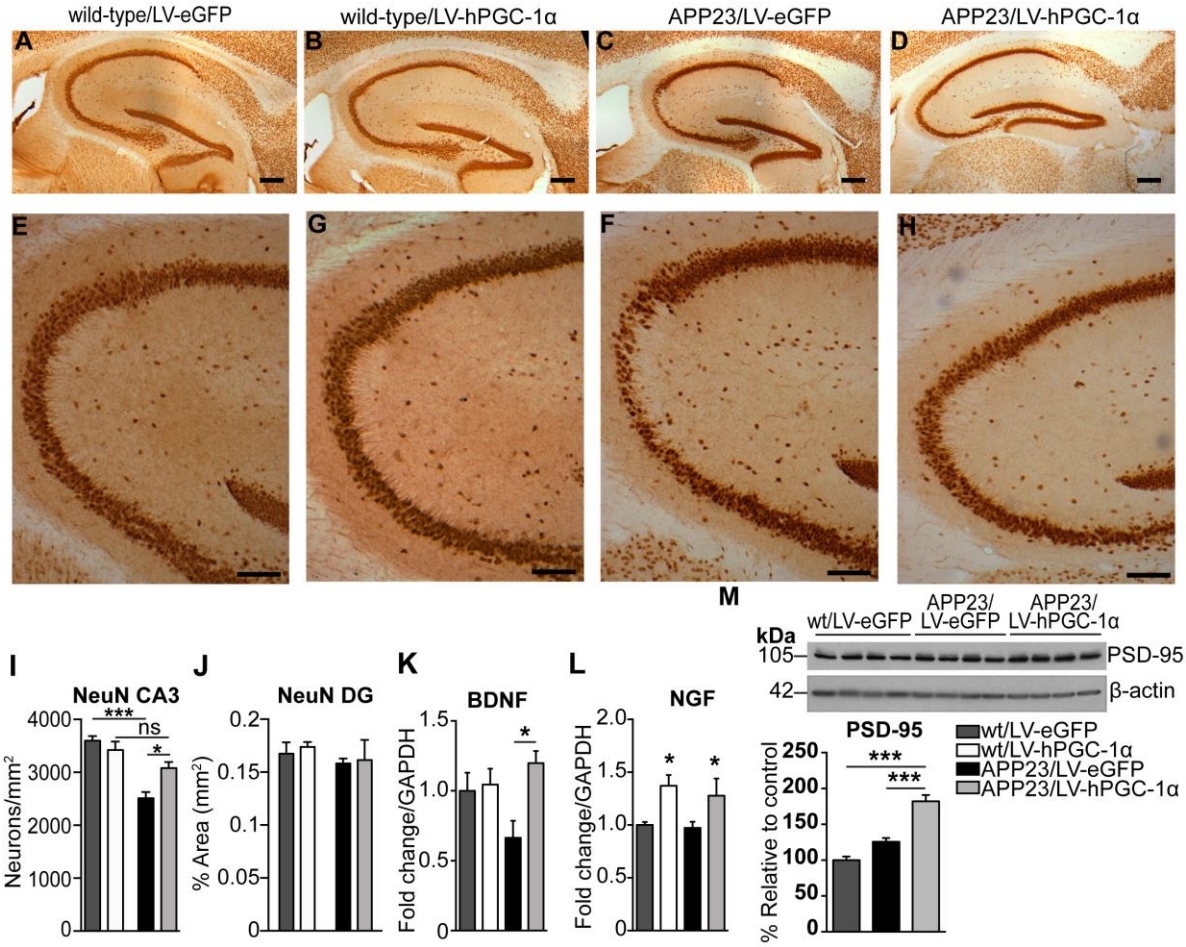

Figure 5.

Attenuation of neuronal loss in the CA3 by hPGC-1α brain gene delivery in APP23 mice. (*A-D*) Representative pictures of NeuN staining in hippocampi of wild-type/LV-eGFP (*A*), wild-type/LV-hPGC-1α (*B*), APP23/LV-eGFP (*C*) and APP23/LV-hPGC-1α injected mice (*D*). Scalebars 0.250 mm. (*E-H*) Higher magnification images of A-D illustrating the striking reduction in neuronal loss in the CA3 area in APP23 mice that received LV-hPGC-1α. Scalebars 0.1 mm. (*I*) Quantification of neuronal

numbers in the CA3 showed a substantial loss of neuronal cells in APP23/LV-eGFP mice compared to wild-type/LV-eGFP which was not observed in APP23 injected with LV-hPGC-1α (n=3-5 per group). Two way ANOVA test (Interaction $F(1,13)= 9.275$, $P= 0.0094$, Treatment $F(1,13)= 2.544$, $P= 0.134$, Genotype $F(1,13)= 34.27$, $P<0.0001$) followed by Bonferroni multiple comparison test. (*K and L*) NGF and BDNF mRNA detected by qRT-PCR were significantly increased in the hippocampi (HIP) of APP23/LV-hPGC-1α injected mice compared to APP23/LV-eGFP. (n= 6 for HIP and n= 5 for Pt Ctx and Ft Ctx). *$P<0.05$, two-tailed Student's t-test. (*M*) Representative western blot and quantification for PSD-95 (n= 5). *$P<0.05$, two-tailed Student's t-test. Data are shown as mean±SEM.

Supporting information PNAS

Three weeks post injection (p.i.) we assessed the transduction efficiency of the virus in areas proximal and distal to the injection site in wild-type mice. Pseudotyping of the HIV-1-based lentiviral vectors with VSVG was not found to be transported to distant areas (Fig S1A-D). In addition, VSVG injections in the hippocampal formation preferentially transduced cells in the dentate gyrus (DG) (Fig S1B and D). Conversely, RVG-CMV resulted in higher expression, transduced cells both proximal and distal to the site of injection and preferentially transduced pyramidal neurons in the cortex and the CA1 area of the hippocampus (Fig S1G-L). This was more relevant for our purpose, because the APP23 mice express hAPP in pyramidal neurons of layers III-V in the cortex and in CA1-3 area in the hippocampus (1). CMV promoter was selected since it resulted in higher expression compared with the SYN promoter (Fig S1E-L, M).

The gene delivery did not affect body weight, which was monitored monthly ($F_{1,37}=0.753$, $P=0.391$, n=9-11; Fig S2B). The performance of the mice in the open field evaluated at one (data not shown) and four months p.i. showed no effect of the treatment or of the genotype on velocity or total distance moved (Fig S2C). Furthermore, thigmotaxis (proximity to walls), reflecting anxiety, was also evaluated in the open field and was observed not to be significantly affected (Fig S2C).

hPGC-1α effect on mitochondrial markers in the brains of APP23 mice

PGC-1α is the master regulator of mitochondrial biogenesis and regulates the level and activity of numerous mitochondrial proteins and enzymes that are essentially involved in major metabolic and respiratory pathways (2, 3). We observed a significant increase in the transcript levels of pyruvate dehydrogenase kinase-1 (*Pdk1*) in the parietal cortex of hPGC-1α treated mice and increased levels of other mitochondrial markers, including COX4, sirtuin-1 and transcription factor A mitochondrial (*Tfam*) in the brains of APP23/LV-hPGC-1α injected mice compared to control APP23/LV-eGFP mice (Fig S5A-J). Other mitochondrial markers were unaltered by the LV-mediated hPGC-1α vector injection. These results suggest that the beneficial effects of the intra-cerebral hPGC-1α gene delivery do not appear to be directly linked to major changes in mitochondrial function or biogenesis.

SI Methods

Lentiviral vectors

The hPGC-1α complete coding sequences with Genbank accession number AF186379 was kindly provided by Dr A. Kralli (The Scripps Research Institute) and the HIV-1 packaging plasmids and pRR-sincppt-CMV-eGFP-WPRE were kindly provided by Professor James Uney (University of Bristol). *hPGC-1α* was subcloned on the lentiviral transfer genome by removing the eGFP cDNA (Suppl. Fig 1B). All vectors carry the woodchuck hepatitis virus posttranscriptional regulatory element (WPRE).

Titration of LV vectors

Biological titre of LV vectors carrying the eGFP reporter gene was determined by flow cytometry as previously described (4). The copy numbers of the viral preparations were determined using the Lenti-X qRT-PCR Titration kit (Clontech) using a Lenti-X RNA known copy number sample to generate a standard curve according to the manufacturer's instructions. The biological titre of LV vectors containing hPGC-1α was extrapolated after calculating the titration ratio of the LV-eGFP (ratio=biological titre/qRT-PCR copies) and by presuming that the two viruses have the same titration ratio, the biological titre was calculated from the formula biological titre=titration ratio/qRT-PCR copies.

Stereotaxic surgeries

Animals were anesthetized (isoflurane 5%, 1L/min O_2) and positioned on a stereotactic frame (World Precision Instruments). Injections were performed bilaterally in the frontal cortex and hippocampus using a 33-gauge blunt needle attached to a 5 ml Hamilton syringe (Hamilton Medical) at 0.2 µl/min (isoflurane 2%, 0.5 L/min O_2 for maintenance of anesthesia). The frontal cortex and the hippocampus were injected with 2.5 µl and 1.5 µl of viral preparation respectively (titre of $1x10^9$ TU/ml). Stereotactic coordinates were calculated from bregma (cortex: AP +2.2 mm, ML ±1.8 mm, DV −3 mm to −0.5 mm, five deposits 0.5 mm apart, 0.5 µl/deposit; hippocampus: AP −2 mm, ML ±1.2 mm, DV −1.5 mm to −1.1 mm, three deposits 0.2 mm apart, 0.5 µl/deposit).

Open Field

Mice were allowed to freely explore a 45x45 cm arena for five min and thigmotaxis, velocity, and total distance moved were assessed using Ethovision XT version 9 software (Noldus).

Object location Test (OLT)

Hippocampal-dependent spatial memory of the mice was tested using the object location test (5) as described previously using a 15 min inter-trial interval (6). This task can assess learning impairment that is attributed mainly to dysfunctional dorsal and CA1 area of the hippocampus (5, 7, 8).

Novel object recognition test (NOR)

Recognition memory of the mice was tested using the novel object recognition test (9, 10). Previous studies have shown that parahippocampal areas of the temporal lobe are involved (9) and the hippocampal formation using a long delay (24h) between training and testing (10). Mice received two days of habituation in a 45x45 cm square arena and on the third day they were allowed to explore two identical objects made from large Lego bricks for 10 min (training trial). They were returned to their home cage, and 24 hours later, a different shape and color object replaced one of the objects and the mice were returned to the arena for 10 min (testing trial). The total time the animal spent exploring each object (characterized by active sniffing or chewing) was recorded using EthoVision XT software (Noldus). The time spent on each object was then calculated as a percentage of total object exploration.

Tissue processing

Mice were deeply anesthetized with pentobarbitone and then transcardially perfused with 30 ml of ice-cold PBS. The brains were rapidly removed, and the right hemisphere was fixed in 4% paraformaldehyde in PBS (0.1 M, pH 7.4) for 48 hours, cryoprotected in 20% sucrose in PBS (0.1 M, pH 7.4), and then sectioned at 35 μm using a vibratome (Leica VT100S). The left hemispheres were dissected, snap frozen, and stored at -80^{o}C until used for biochemical analyses.

Immunohistochemistry and immunofluorescence

Sections were treated for 20 min with 0.6% H2O2 in TBS, permeabilized in TBS-Triton X-100 0.25% (TBS-Tx) for 30 min, and blocked for one hour with 10% fetal bovine serum (FBS) in TBS-Tx 0.1%.

For Aβ staining, an additional step of antigen retrieval with 98% formic acid was performed before permeabilization.

Image analyses

For assessing amyloid and plaque burden, the percentage of the area covered by Aβ or AmyloGlo staining was calculated using the NIH ImageJ software (seven sections per animal, n=9) as previously described (6). To obtain measures of Aβ-associated microgliosis and astrocytosis, 50 μm^2 and 100 μm^2-diameter circles respectively were centered over plaques to define plaque domains and then superimposed on images of Iba1-stained microglia and GFAP-stained astrocytes. Fluorescent intensities were calculated within each plaque domain in at least three plaques per section and expressed as mean grey area (corresponding to mean pixel intensity, four sections per animal, n=5). Additionally, the extent of plaque-associated microgliosis and astrocytosis was analyzed by thresholding the images and measuring the % of area occupied by Iba1- and GFAP-positive cell bodies and processes within individual plaque domains, serving as indication of the number of cells bodies around the plaques (11). For neuronal cells quantifications we measured the number of positive cells in three random squares 150x150μm for subiculum, and 100x100 μm for CA3 and the area occupied by the dentage gyrus as previously described15.

Western blotting

Mouse brain samples were homogenized in radioimmunoprecipitation assay buffer (1% Triton X-100, 1% sodium deoxycholate, 0.1% SDS, 150 mM NaCl, and 50 mM Tris-HCl, pH 7.2) supplemented with protease and phosphatase inhibitors (Roche).

Determination of soluble-APP (sAPPα and sAPPβ) and APP carboxy-terminus domains (CTFs)

To determine soluble APP and αCTFs in brain homogenates, 50 μg were pulled down overnight at 4ºC using Sepharose Protein A (Zymed, US) and 140, a polyclonal antibody recognising the CT-domain of APP (from Jochen Walter, University of Bonn) in order to immunoprecipitate full length APP. Samples were then spun down and pellets were then loaded in NuPage 4-12% Tris-glycine gels and transferred onto nitrocellulose membranes and incubated with R1-57 antibody for CTFs determination.

Supernatants were run in 10% SDS gels and incubated with 6E10 antibody at 1/1000 (a monoclonal antibody recognising amino acids 1-17 of human Aβ (Covance, US)) for sAPPα and with an antibody against sAPPβ from Millipore.

Primers used in qRT-PCR

Bace1 (QT00493948) Quantitect Primer assays from Qiagen; Adam10 (Mm00545742_m1), Adam17 (Mm00456428_m1), Bdnf (Mm432069_m1), Foxo1 (Mm00490672_m1), Gapdh (Mm99999915_g1), Ide (Mm00473077_m1), Mme/Nep (Mm00485028_m1), Nrf1 (00447996_m1), PPARGC1A/PGC-1A (Hs01016719_m1), Pdk1 (Mm00554306_m1), Sirt1 (Mm01168521_m1), Tfam (Mm00447485_m1), Taqman gene expression Assays from Applied Biosystems; Aco2 (for: 5'-TGATGCAAACCCTGAGACC-3', rev: 5'-GAGCCTCCAACTTGAACTTCT-3'), ApoE (for: 5'-CTGACAGGATGCCTAGCCG-3', rev: 5'-CGCAGGTAATCCCAGAAGC-3'), Cox6 (for: 5'-TCATATTGCTGGCGCATTC-3', rev: 5'-CCTTCCTCATCTCTTCGAAATC-3'), CS (for: 5'-CCAATCTGCACCCTATGTCTC-3', rev: 5'-GTCCATGCAGTCCTCATAGATG-3'), Gapdh (for: 5'-ACCACAGTCCATGCCATCAC-3', rev: 5'-TCCACCACCCTGTTGCTGTA-3'), Ngf (for: 5'-CCAGTGAAATTAGGCTCCCTG-3', rev: 5'-CCTTGGCAAAACCTTTATTGGG-3') and Pfk (for: 5'-AAGTCTGCCATCACCTGACC-3', rev: 5'-TCCCACAAGACATACACATGG-3'), custom-made from Sigma-Aldrich UK.

SI References

1. Sturchler-Pierrat C, et al. (1997) Two amyloid precursor protein transgenic mouse models with Alzheimer disease-like pathology. *Proc Natl Acad Sci* 94(24):13287–13292.
2. Puigserver P, Spiegelman BM (2003) Peroxisome proliferator-activated receptor-gamma coactivator 1 alpha (PGC-1 alpha): transcriptional coactivator and metabolic regulator. *Endocr Rev* 24(1):78–90.
3. Austin S, St-Pierre J (2012) PGC1α and mitochondrial metabolism--emerging concepts and relevance in ageing and neurodegenerative disorders. *J Cell Sci* 125(Pt 21):4963–71.
4. Eleftheriadou I, Trabalza A, Ellison S, Gharun K, Mazarakis N (2014) Specific retrograde transduction of spinal motor neurons using lentiviral vectors targeted to presynaptic NMJ

receptors. *Mol Ther* 22(7):1285–98.

5. Moser E, Moser MB, Andersen P (1993) Spatial learning impairment parallels the magnitude of dorsal hippocampal lesions, but is hardly present following ventral lesions. *J Neurosci* 13(9):3916–25.
6. Katsouri L, et al. (2015) Systemic administration of fibroblast growth factor-2 (FGF2) reduces BACE1 expression and amyloid pathology in APP23 mice. *Neurobiol Aging* 36(2):821–31.
7. Assini FL, Duzzioni M, Takahashi RN (2009) Object location memory in mice: Pharmacological validation and further evidence of hippocampal CA1 participation. *Behav Brain Res* 204(1):206–211.
8. Nakazawa K, McHugh TJ, Wilson M a, Tonegawa S (2004) NMDA receptors, place cells and hippocampal spatial memory. *Nat Rev Neurosci* 5(5):361–372.
9. Dere E, Huston JP, De Souza Silva M a. (2007) The pharmacology, neuroanatomy and neurogenetics of one-trial object recognition in rodents. *Neurosci Biobehav Rev* 31(5):673–704.
10. Hammond RS, Tull LE, Stackman RW (2004) On the delay-dependent involvement of the hippocampus in object recognition memory. *Neurobiol Learn Mem* 82(1):26–34.
11. Rodriguez GA, Tai LM, LaDu MJ, Rebeck GW (2014) Human APOE4 increases microglia reactivity at Abeta plaques in a mouse model of Abeta deposition. *J Neuroinflammation* 11(1):111.

SI Figures

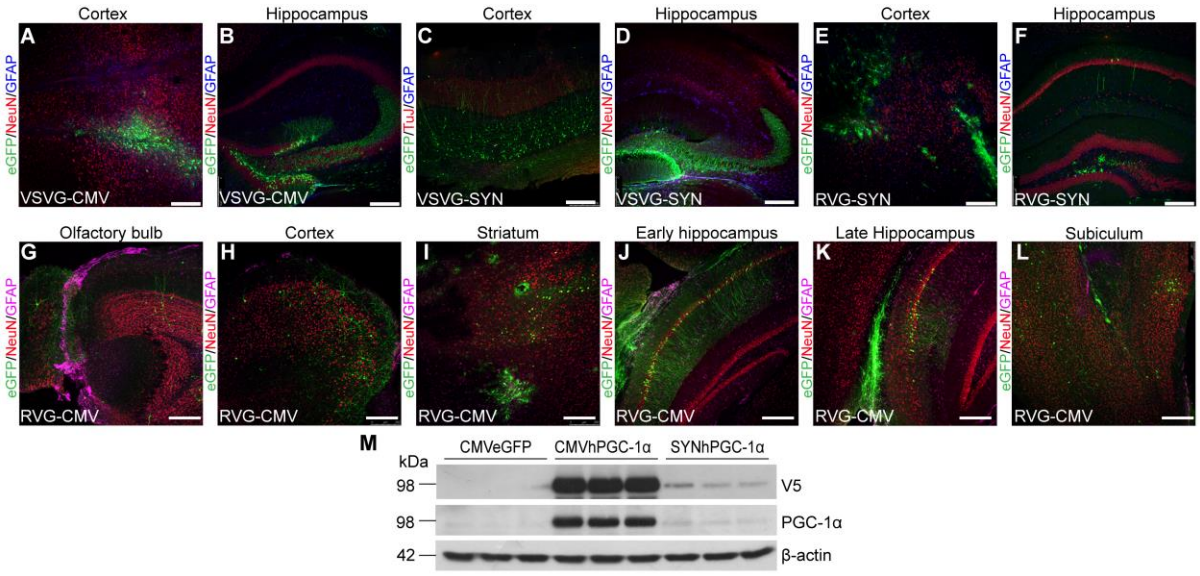

Figure S1.

Expression analysis of viral envelope glycoproteins and promoters. (*A-L*) Different glycoproteins and promoters were trialed with lentiviral vectors and their biodistribution was examined three weeks post-stereotaxic delivery in the frontal cortex and hippocampus of wild-type mice. Expression was confirmed in several brain areas both proximal and distal to the injection sites (n=3, 16-20 sections). Scalebars 250µm. (*M*) HEK293T cells were transfected with the transfer genome plasmid for CMV-eGFP, CMV-hPGC-1α and SYN-hPGC-1α respectively. Representative western blots of cell lysates for the V5 tag of hPGC-1α and β-actin as loading control.

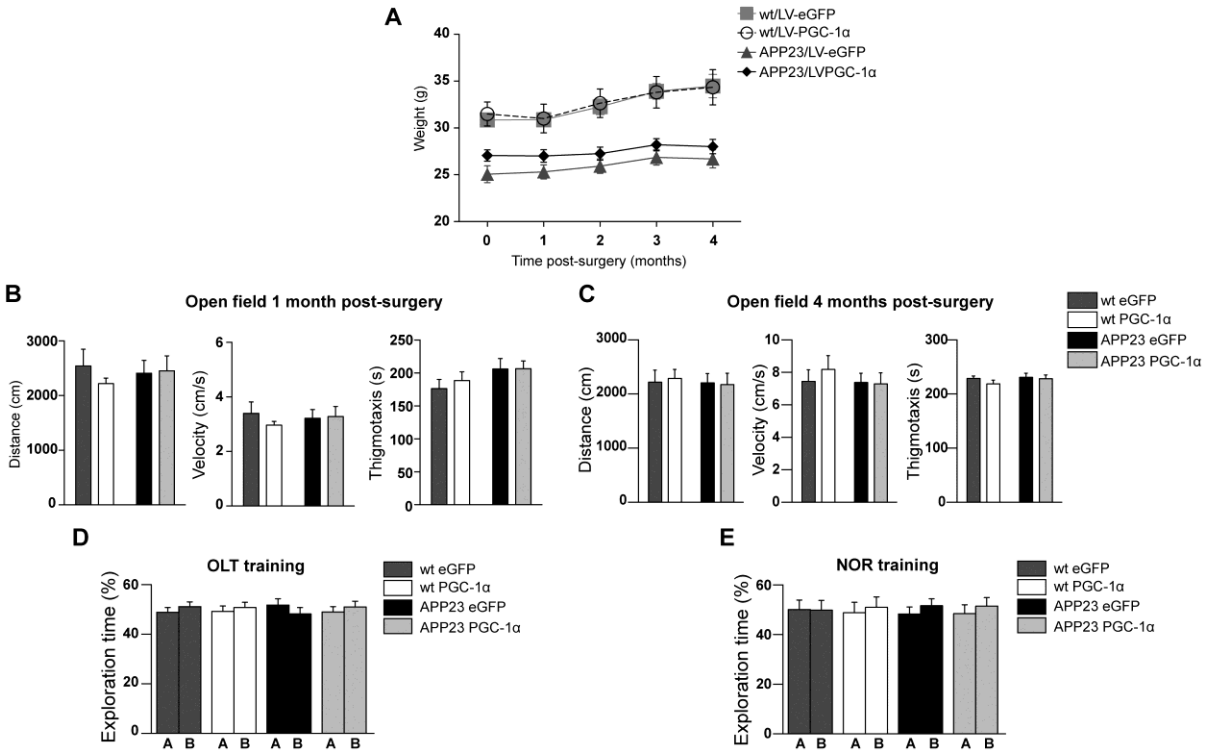

Figure S2.

(*A*) Monthly weight monitoring showed no effect between the two viral vectors on body weight (two-way repeated measures ANOVA F1,37=0.753, P=0.391, n=9 to 11). (*B*) Open field performance one month post-surgery showing no difference between the four groups of mice (two-way ANOVA followed by Bonferroni post-test; Distance moved: Genotype $F_{(1,37)}$= 0.0066, *P*= 0.9358, Treatment $F_{(1,37)}$= 0.071, *P*= 0.7917; Velocity: Genotype $F_{(1,37)}$= 0.0071, *P*= 0.9332, Treatment $F_{(1,37)}$= 0.072, *P*= 0.7916; Thigmotaxis: Genotype $F_{(1,37)}$= 2.902, *P*= 0.0968, Treatment $F_{(1,37)}$= 0.2056, *P*= 0.6529; n= 9 to 11). (*C*) Open field performance four months post-surgery (two-way ANOVA followed by Bonferroni post test; Distance moved: Genotype F(1,37)= 0.107, P= 0.652, Treatment F(1,37)= 0.01, P= 0.921; Velocity: Genotype F(1,37)= 0.444, P= 0.510, Treatment F(1,37)= 0.207, P= 0.652; Thigmotaxis: Genotype F(1,37)= 0.744, P= 0.395, Treatment F(1,37)= 0.855, P= 0.361; n= 9 to 11). (***D***) OLT training session showing no preference for object A or B. (***E***) Mice explored the two objects equally during the NOR training session.

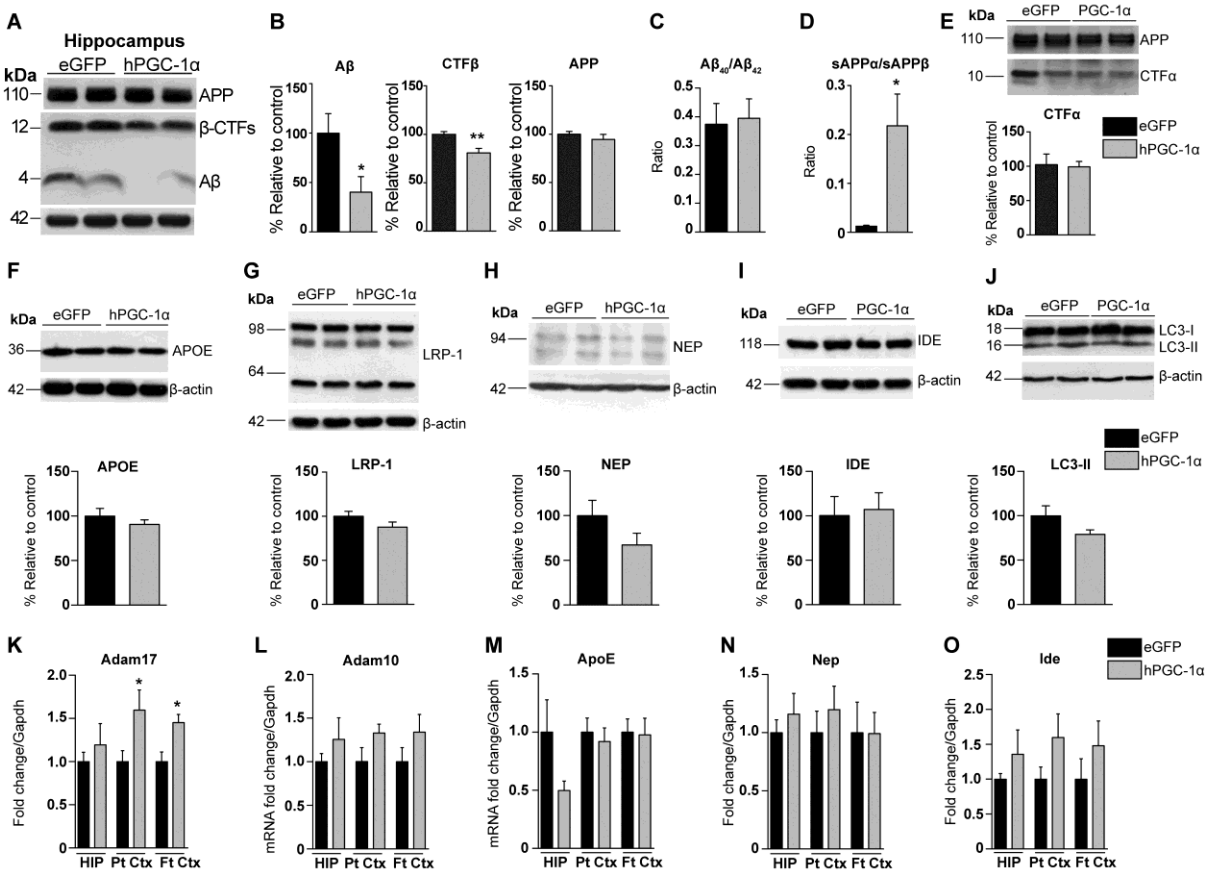

Figure S3.

hPGC-1α overexpression does not alter Aβ clearance or degradation (*A-D*) Chronic overexpression of LV-hPGC-1α did not alter the expression of APOE and its receptor LRP-1 (A and B) or the Aβ degrading enzymes neprilysin and IDE (*C and D*) (n= 5, two-tailed Student's *t-test*). APOE, apolipoprotein E; LRP-1, low-density lipoprotein receptor-related protein 1; NEP, neprilysin; IDE, insulin-degrading enzyme. (*E*) No changes were detected in autophagy by western blotting for LC3 between LV-eGFP and LV-PGC-1α injected APP23 mice. (*F-I*) The mRNA levels of Adam10, ApoE, Nep and Ide remained largely unaffected by the hPGC-1α LV injection (n= 6 for HIP, n=7 for Pt Ctx and n=5 for Ft Ctx, two-tailed Student's *t-test*). Data are shown as mean±SEM.

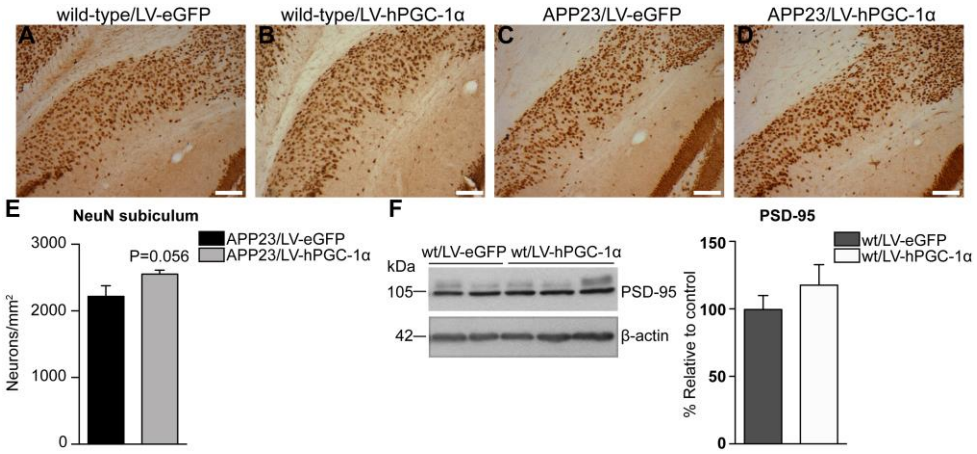

Figure S4.

Neuronal cell density in subiculum of animals injected with LV-hPGC-1α or LV-eGFP. (*A-D*) Representative images of the subiculum where no changes were detected between LV-eGFP (A, wild-type; C, APP23) and LV-hPGC-1α injected mice (B, wild-type; D, APP23). Scalebars 0.1 mm (n= 3 for wild-type and n= 5 for APP23, 6 sections per mouse). (*E*) Quantification of NeuN+ cells in the subiculum of APP23 mice injected with LV-eGFP or LV-hPGC-1α showed no significant differences in the neuronal numbers (n= 5, 6 sections per mouse, two-tailed Student's t-test). Data are shown as mean±SEM.

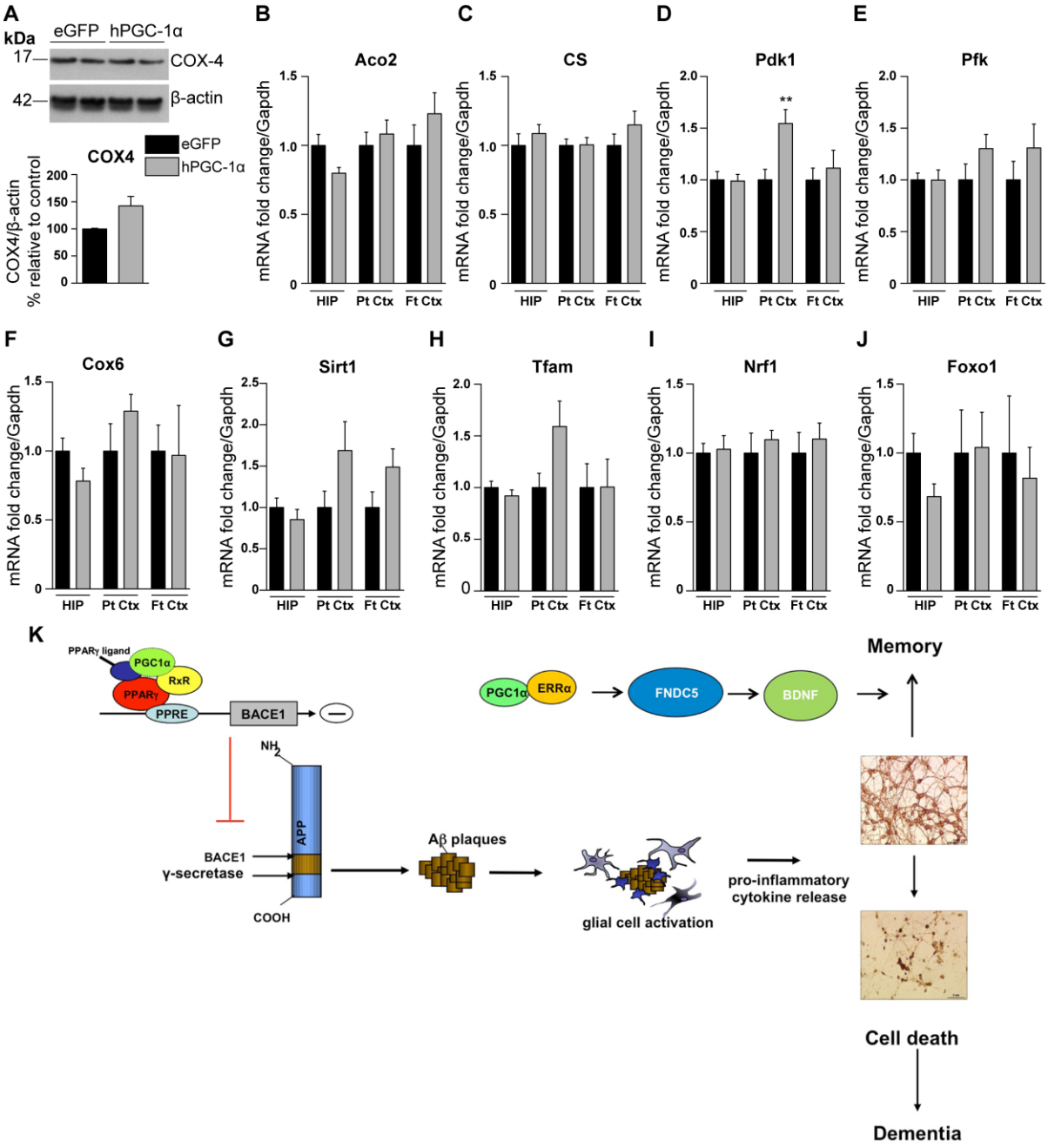

Figure S5.

Quantification of the expression of mitochondrial markers in brains of APP23/LV-hPGC-1α mice compared to APP23/LV-eGFP. (*A*) Representative western blot of COX-4 (two animals from each group shown here) and its quantification (n= 5, two-tailed Student's t-test). (*B-F*) The mRNA expression of the mitochondrial markers Aco2 (*B*), CS (*C*), Pfk (*E*), and Cox6 (*F*) appears to be unaltered. There was a significant increase of Pdk1 (*D*) in the parietal cortex which was the area that had the highest expression of hPGC-1α (**P<0.01, two-tailed Student's t-test). (*G-J*) qRT-PCR for Sirt1 (*G*), Tfam (*H*), Nrf1 (*I*), and Foxo1 (*J*) showed that LV-hPGC-1α did not change their expression.

(HIP; n= 6), parietal cortex (Pt Ctx; n= 7) and frontal cortex (Ft Ctx; n= 5). Cox-4 = cytochrome c oxidase subunit IV, Aco2= aconitase 2, CS= citrate synthase, Pdk1= pyruvate dehydrogenase kinase, Pfk= phosphofructokinase, Cox-6= cytochrome c oxidase subunit VI, Sirt1= sirtuin 1, Tfam= transcription factor A mitochondrial, Nrf1= nuclear respiratory factor 1, Foxo1= forkhead box O1. Data are shown as mean±SEM and all samples were run in duplicates. (*K*) Schematic model showing the mechanistic effects of PGC-1α gene therapy in AD, by affecting BACE1 transcription-leading to reduced Aβ generation and neuroinflammation and increasing the expression of neurotrophic growth factors.